Available online at www.sciencedirect.com

ScienceDirect

journal homepage: www.elsevier.com/locate/he

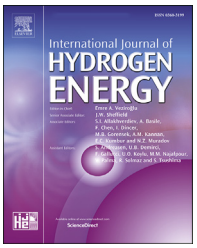

An advanced control method for fuel cells - Metal hydrides thermal management on the first Italian hydrogen propulsion ship

M. Cavo, M. Rivarolo[*], *L. Gini, L. Magistri*

Thermochemical Power Group (TPG), DIME, University of Genoa, Via Montallegro 1, 16145 Genoa, Italy

HIGHLIGHTS

- Integration of PEMFC and metal hydrides (MH) for zero-emissions ship is presented.
- A Matlab-Simulink model is developed for the PEMFC and MH systems.
- Two control systems (PID, MPC) are investigated for strong energy load variations.
- Three possible solutions are presented to avoid problems to PEMFC in transients.
- The MPC results the best solution to avoid thermal stress on PEMFC.

ARTICLE INFO

Article history:
Received 31 March 2022
Received in revised form
17 June 2022
Accepted 26 July 2022
Available online xxx

Keywords:
Hydrogen
PEM fuel Cells
Metal hydrides
Energy systems modelling
Marine transportation

ABSTRACT

As International Maritime Organization set 2030 and 2050 targets to reduce CO2 emissions in maritime sector, the investigation of innovative clean solution as hydrogen fuel cells for clean energy generation onboard is gaining more and more value.

The present study investigates the thermal integration between PEM fuel cells and metal hydrides (for hydrogen storage) on board the first Italian zero-emissions ship with hydrogen and batteries propulsion, named ZEUS, built by Fincantieri Yard and launched in 2022. A model-based approach is developed to ensure the system's control at different load demands for the vessel, including transient conditions. The study focuses on the most critical conditions for fuel cells during navigation, namely from maximum to minimum power and vice-versa. Load reduction does not imply particular issues, while load maximum increase may cause some problems in terms of stability, negatively affect fuel cell stacks lifetime. Three solutions are investigated and compared to solve the problem to achieve a safe and robust control system: (i) decrease the current ramp for fuel cells from 50 to 10 A/s; (ii) introduce an intermediate load step; (iii) adopt an advanced Model Predictive Control strategy.

* *Corresponding author.*
E-mail address: massimo.rivarolo@unige.it (M. Rivarolo).

https://doi.org/10.1016/j.ijhydene.2022.07.223

Nomenclature

Acronyms

DLQR	Discrete Linear Quadratic Regulator
DMPC	Discrete Model Predictive Control
ECA	Emission Control Area
FCS	Fuel Cell Systems
GHG	Green House Gases
HiL	Hardware in the Loop
ICE	Internal Combustion Engine
IEA	International Energy Agency
IMO	International Maritime Organization
LNG	Liquefied Natural Gas
MH	Metal Hydrides
MPC	Model Predictive Control
NMSS	Non-Minimal State Space
PEMFC	Polymer Electrolyte Membrane Fuel Cell
PID	Proportional-Integrative Derivative
PMS	Power Management System
RES	Renewable Energy Sources
SiL	Software in the Loop
SoC	State of Charge
TPG	Thermochemical Power Group
WGHE	Water-Glycol Heat Exchanger
WSHE	Water-Sea Water Heat Exchanger
ZEUS	Zero Emission Ultimate Ship

Symbols

E	Electrical energy [kWh]
H	Pump Head [m]
J	DLQR cost function
N	Number of modules
P	Power [kW]
R	MPC weight matrix
Q	Heat [kW] or MPC weight matrix
TT	Temperature transmitter
u	Control signal
x	State vector of NMSS system
y	Output of NMSS system
η	Efficiency

Introduction

It is a matter of fact that CO_2 emissions are dramatically increasing more and more: in 2019, the record value of 33.5 Gt was reached and in 2021, after a reduction due to pandemic effect in 2020 (31.5 Gt), they have increased again up to 33.0 Gt [1]. Referring to 2019 IEA data [2], energy producers represent the main CO_2 emissions' sector (14.2 Gt), followed by transport (8.2 Gt) and industry (6.2 Gt). Among transports, the maritime transportation sector has a significant impact: the 4th report by International Maritime Organization (IMO) estimates an increasing trend in CO_2 emissions, from 962 Mt in 2012 up to 1056 Mt in 2018 [3]. Considering that almost the totality (>98%) of the ships in operation employ fuel products derived by oil (Marine Diesel Oil and Marine Fuel Oil) in Internal Combustion Engines (ICEs) for propulsion and energy generation onboard, their pollutant impact is high [4], also in terms of PM, NOx and SOx emissions. The IMO already implemented several regulations in the last years, reducing the allowed level of SO_x and NO_x emissions, with more stringent limitation in Emission Control Areas (ECAs) in particular. More recently, IMO also set long-term targets to cut 50% GHG emissions by 2050, compared to 2008 [4–6]. To reach this goal, different strategies are possible, including installation of renewable energy systems (RES) onboard [7], use of low-impact alternative fuels [8–10] and energy efficiency increase to reduce fuel consumptions, e.g., designing vessels with low resistance [11,12]. According to many studies [5,6], the introduction of low-environmental impact fuels and innovative technologies for maritime transport represents a key point. Among the potential alternative fuels, methanol, and LNG [13,14] represent worthy solutions to minimize SOx and NOx, at the same time reducing the impact in terms of carbon dioxide: however, they are not carbon free, thus they are not sufficient to meet the long-term targets established by IMO related to CO_2. Ammonia and hydrogen, in particular if produced by RES, may represent two valuable solutions for shipping [15–17], as their CO_2 emissions are zero.

Fuel Cell Systems (FCS) represent an interesting technology for maritime applications [18–20], as they have high efficiency, low noise and vibrations and low pollutant emissions. Recent literature reports many possible fuel cells' use in maritime field as an alternative to ICE, up to 1 MW size [22–24]. Among the existing FCS, Proton Exchange Membrane Fuel Cells (PEMFC), fed by high purity H_2, currently represent the most promising technology, thanks to the compactness, the quick answer to load variations and their zero impact in terms of pollutant or CO_2 emissions [22,25]. This opened the research to investigate solutions for the modelling of PEMFC and hybrid systems, considering the coupling with electrical batteries onboard [26–28], also considering their behavior for transient and dynamic conditions [28–31]; in parallel, several experimental analyses on laboratory scale test rigs were developed [32–34].

A key-point related to PEMFC utilization for sustainable transports is due to the high volumes related to H_2 storage. Nowadays, the most employed methods for hydrogen storage consist of pressurized tanks (200–800 bar) or cryogenic vessels for liquid storage (at −253 °C), but both the methods require significant volumes onboard and high energy demand for the storage [35,36]. Metal Hydrides (MH) can represent a worthy solution, as they allow for good energy storage in volume terms, without needing the considerable energy input required for the above-mentioned methods, as hydrogen is stored at limited pressure (<40 bar) and temperature (<100 °C) [37,38]. It must be noted that storing hydrogen in MH has a significant drawback in weight terms; however, in case of ships, this aspect can be limited by properly positioning MH tanks onboard [39,40]. The thermal coupling of PEMFC and MH has been investigated by several authors in the last years: as H_2 release from MH storage is an endothermal reaction, the needed thermal energy input can be recovered from the PEMFC, as investigated in Refs. [41–43].

In the last years, many prototype and research vessels for the utilization of PEMFC onboard (size up to 200 kW) have been successfully demonstrated [44–46]. Very recently Fincantieri, together with Isotta Fraschini Motori S. p.A and granted by the Italian Ministry of Economic Development (MISE) in the *TecBia*

Please cite this article as: Cavo M et al., An advanced control method for fuel cells - Metal hydrides thermal management on the first Italian hydrogen propulsion ship, International Journal of Hydrogen Energy, https://doi.org/10.1016/j.ijhydene.2022.07.223

research project, has developed and built the first Italian H_2 propulsion ship, named Zero-Emission Ultimate Ship (*ZEUS*), in operation since 2022 and fully powered by PEMFCs (two branches, 71 kW each) and electric batteries (nearly 160 kW) [47]. The choice of installing PEMFC for the ZEUS vessel is due to many reasons, such as their availability on the market for the required size (higher than 100 kW), the possibility of zero-emissions propulsion and the fast response in transient (not possible with different FCS, such as high temperature ones). The hydrogen is stored onboard in MH, for a total amount of 50 kg. The *TecBia* project is going to be completed by the end of 2022 with tests in open sea for different navigation conditions. The integration between the fuel cells and the hydrogen storage system and the control system represent two key points for the ZEUS optimal management.

In previous research, the authors developed a control system for the PEMFC-MH system management installed onboard throughout a model-based approach and tested the dynamic behavior for different operating conditions for the ZEUS vessel [43]. More in detail, the authors validated the model with data from PEMFC and MH producers and tested the integrated system, verifying that the heat produced by the PEMFC was sufficient to release the needed H_2 amount from the MH installed on-board for the cruise speed of 6 knots and the required autonomy (7 h). However, in such kind of applications the optimization of the control strategy to answer to fast and high load variations (i.e., from minimum to maximum power and vice-versa) is mandatory, also considering that PEMFC represent the propulsion system onboard, integrated with electrical batteries; an excessive stress would reduce their lifetime, with dramatic consequences also from the economic standpoint.

The aim of this paper is to test the thermal management loop of the PEMFC + MH propulsion system mounted onboard the ZEUS vessel. The dynamics of each control element must be investigated to verify the capability to bring the system to the desired equilibrium point avoiding the exposition of PEMFC to extended critical operations: this is fundamental to preserve the FCS' lifetime. A dynamic model in Matlab Simulink environment has been developed and validated for this purpose. The simulations are computed to cover the most stressful operating ramps: from minimum power to nominal power and vice versa. Different plant solutions for managing the control devices are analysed according to the manufacturer's suggestions and the most modern control tools.

System description and model approach

The thermal management system of the PEMFC and MH units installed on the ZEUS is shown in Fig. 1. The system includes two parallel generation branches consisting of two PEMFC modules. In each branch (first loop, red line) a cooling flow constituted by water and glycol (50-50 mixture) circulates, driven by a pump (P1/P2); an expansion vessel (ET) and three-way partition valves ($V1_{A/B}$ and $V2_{A/B}$) are also installed. A water-based metal hydride heating system, consisting of a motion pump (P0), metal hydride racks, a three-way shut-off valve (V0) and three heat exchangers (WGHE-1/2 and WSHE), is located at the bottom (second loop, green line). The FCS cooling circuits are coupled to the MH heating circuits through two water-glycol heat exchangers (WGHE1 and WGHE2). The heat produced by the operating PEMFCs activates the hydrogen release reactions of the MH metal powder. The eventual excess heat is dissipated through the water-sea heat exchanger (WSHE), which uses seawater as cold source. Depending on the system's operative conditions, it is necessary to properly manage the heat dissipation in WSHE with the controlled by-pass valve V0.

A Matlab Simulink model (Fig. 2) is developed to study the dynamic behavior of the thermal management system of the FCS installed on the ZEUS. The main components involved in the coupling of PEMFC modules cooling system and MH racks are modelled. The aim is to represent the dynamics of the complete system to investigate the effects of different control strategies on the power generation modules. Each model solves the main thermodynamic fluid dynamics governing equations; the mathematical description of the main modules (PEMFC, MH, WGHE, WHSE, three-way valves, pumps) was presented in detail in previous authors' publication [43]. Table 1 reports the most significant equations for the different components.

A simplified battery model is integrated to evaluate energy consumption due to PEMFC dynamics. This is described by equation (1); battery discharge efficiency $\eta_{bat,disch}$ is assumed constant.

$$\frac{d\,(\mathrm{SoC_{bat}})}{dt} = -\frac{P_{disch}}{E\,N_{bat}}\eta_{bat,disch} \tag{1}$$

Both branches are modelled, although their behavior is expected to be the same. The purpose of this choice is to allow future investigations of transient operating phases from partial load (one branch switched on) to full load (both branches switched on). In this study, the system is assumed to operate at full load. Table 2 reports the main data for the different systems installed onboard ZEUS vessel and considered in this paper. PEMFC, MH and battery energy systems are produced by ProtonMotor [48], GKN [49] and Valence [50] manufacturers respectively.

Control strategy

When an increase in load demand occurs, the Power Management System (PMS) acts on the PEMFC modules by increasing the current supplied to meet the net electrical demand. The efficiency of FCS decreases as the current increases; thus, the amount of heat required to ensure stable operation of the modules increases significantly. In this paper two current rates are analysed: 50 A/s and 10 A/s. The control strategy is designed to meet the requirements of the PEMFC modules manufacturer. The main constraints that must be complied by the thermal management system are the water-glycol outlet temperature from fuel cells modules for each operating branch ($TT11_{A/B}$ and $TT21_{A/B}$ in Fig. 1) and the water-glycol outlet temperature of interface heat exchanger (WGHE1/2) for each operating branch (TT12 and TT22 in Fig. 1). Table 3 shows the temperature set points at different working conditions.

$V1_{A/B}$ and $V2_{A/B}$ three-way valves are designed to ensure the thermal requirement at the stack outlet (first loop), bypassing part of the flow destined to the water-glycol heat exchanger (WGHE). Therefore, when an increase of stack load

Please cite this article as: Cavo M et al., An advanced control method for fuel cells - Metal hydrides thermal management on the first Italian hydrogen propulsion ship, International Journal of Hydrogen Energy, https://doi.org/10.1016/j.ijhydene.2022.07.223

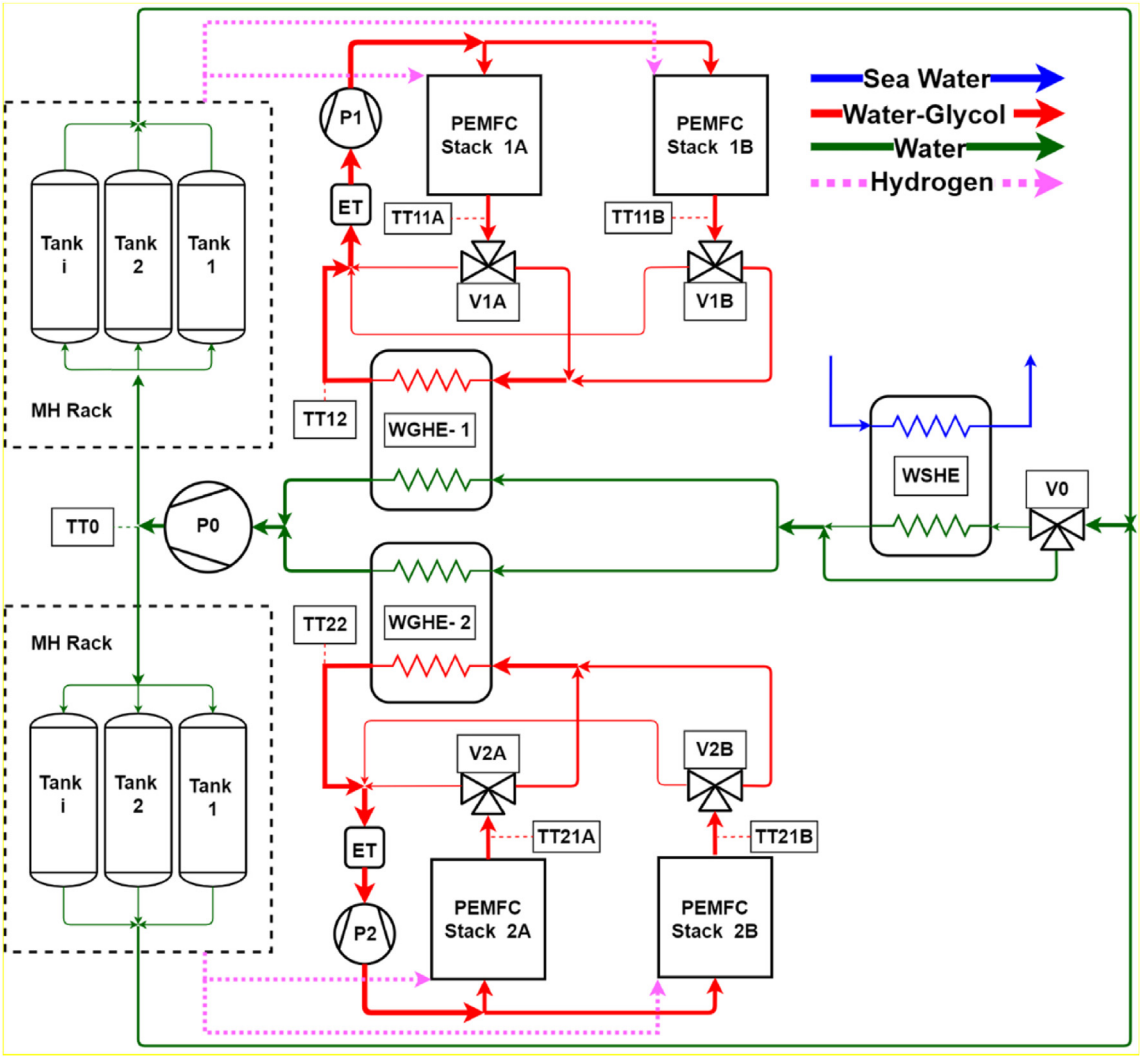

Fig. 1 – Simplified layout of ZEUS thermal system loop.

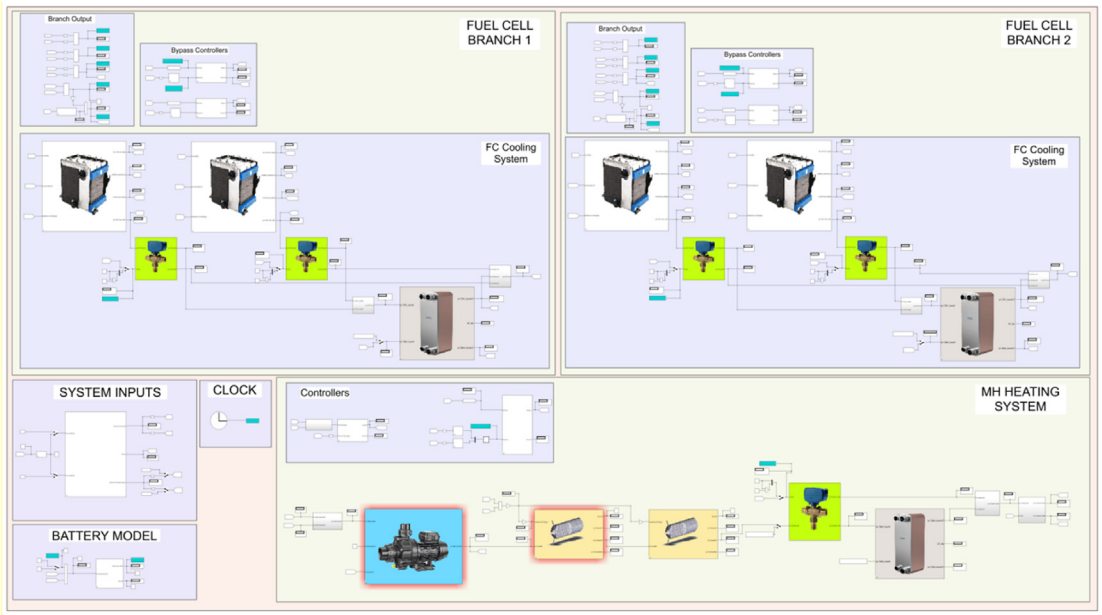

Fig. 2 – Dynamic model of ZEUS thermal management system.

Please cite this article as: Cavo M et al., An advanced control method for fuel cells - Metal hydrides thermal management on the first Italian hydrogen propulsion ship, International Journal of Hydrogen Energy, https://doi.org/10.1016/j.ijhydene.2022.07.223

Table 1 – Main components' equations of the thermal management system installed on ZEUS ship [43].

PEMFC model

$$V_{cell} = 1.229 - 0.85\,10^{-3}(T_{st} - 298.15) + \frac{R}{2F}T_{st}\left[\ln(p_{H_2}) + \frac{1}{2}\ln(p_{O_2})\right] - V_{act} - V_{ohm}$$

$$Q_{ST} = (V_{act} + V_{ohm})\,i\,n$$

$$P_{el} = (i\,V_{cell})n$$

$$Q_{exch} = Q_{max}\,\varepsilon$$

$$\frac{dT_{out,COOL}}{dt} = \frac{1}{M_{COOL}\,c_{p_{COOL}}}(\dot{m}_{COOL}c_{p_{COOL}}(T_{in,COOL} - T_{out,COOL}) + Q_{exch})$$

$$\dot{m}_{H_2,\,stech} = n\frac{i}{2F}MM_{H_2}$$

$$P_{el,NET} = P_{el}\,\eta_{DC/DC} - BoP$$

MH model

$$\left(\frac{v_{tank}}{v_{MH}} - 1 + e\right)\frac{d\rho_g}{dt} = -n_d - \frac{\dot{m}_{H_2,out}}{v_{MH}}$$

$$n_d = C_d exp\left(\frac{-E_d}{RT_{MH}}\right)\left(\frac{p_g - p_{eq}}{p_{eq}}\right)\left(\rho_s - \rho_0\right)$$

$$\nu_{MH}(e\rho_g c_{p_g} + (1-e)\rho_s c_{p_s})\frac{\partial T_{MH}}{\partial t} = K_e\nabla^2 T_{MH} + Q + S_{TH}$$

WGHE and WSHE models

$$Q_{exch,HOT,j} = U_{HOT}\frac{A_{HOT}}{N}(T_{HOT,j} - T_{METAL,j})$$

$$Q_{exch,HOT,j} = U_{HOT}\frac{A_{HOT}}{N}(T_{HOT,j} - T_{METAL,j})$$

$$Q_{exch,METAL,j} = k\frac{N}{L}A_{METAL}(T_{METAL,j-1} - T_{METAL,j}) + k\frac{N}{L}A_{METAL}(T_{METAL,j+1} - T_{METAL,j})$$

$$\frac{dT_{HOT,j}}{dt} = \frac{N}{M_{HOT}\,c_{p_{HOT}}}(\dot{m}_{HOT}c_{p_{HOT}}(T_{in,HOT,j} - T_{HOT,j}) - Q_{exch,HOT,j})$$

$$\frac{dT_{COLD,j}}{dt} = \frac{N}{M_{COLD}\,c_{p_{COLD}}}(\dot{m}_{COLD}c_{p_{COLD}}(T_{in,COLD,j} - T_{COLD,j}) + Q_{exch,COLD,j})$$

$$\frac{dT_{METAL,j}}{dt} = \frac{N}{M_{METAL}c_{p_{METAL}}}(Q_{exch,METAL,j} + Q_{exch,HOT,j} - Q_{exch,COLD,j})$$

Pump model

$$\dot{Q} = \frac{H_0}{H_{nominal}k} - \left(\frac{H}{H_{nominal}k}\right)\frac{1}{3}$$

$$where\,\frac{H_0}{H_{nominal}} = 160\,\%\;and\;k = 1.6\cdot10^{-4}$$

Three-Way Valves models

$$\dot{m}_{OUT,1} = \dot{m}_{IN}\frac{OF}{100}$$

$$\dot{m}_{OUT,2} = \dot{m}_{IN} - \dot{m}_{OUT,1}$$

occurs, it is reasonable to expect a drop in the bypassed mass fraction. Similarly, the V0 valve increases the water flow through the WSHE to guarantee the water-glycol set point temperature (second loop) at WGHE outlet. However, the simulations will show that a temporary increase of the mass fraction bypassing the heat exchangers is useful to overcome the thermal dynamics of the system. In fact, the heating phenomenon of the vector fluids is delayed by the inertia of the circuit; therefore, it is necessary to decrease provisionally the flow through the exchangers to avoid a sudden system cooling. This result is relevant as it is not achievable through a static analysis of the system and can be crucial in structuring a stable and fast control system on the ship. In order to simulate valve control systems, two approaches are analysed: the Proportional Integral Derivative (PID) method and the Model Predictive Control (MPC) method.

PID controller

PID control is a typical control algorithm with a huge usage in industry applications, including fuel cell systems [52–55]. Its popularity is attributed to a wide range of operating conditions and to its functional and implementation simplicity. It consists of three basic coefficients: proportional (K_P), integrative (K_I), and derivative (K_D). They are varied to get an optimal response of the control variable ($u(t)$); so, the basic idea behind PID controller is to read a sensor, evaluate the error between the control variable and the required set point ($e(t)$) and generate the desired actuator output summing the proportional, integrative and derivative responses (Fig. 2) as equation (2) reports.

$$u(t) = K_P e(t) + K_I\int e(\tau)d\tau + K_D\frac{d\,e(t)}{dt} \quad (2)$$

In order to obtain a stable controller, it is necessary to tune the characteristic constants of the PID. There are two control loops in the ZEUS ship's PEMFC and metal hydrides thermal management system. The first loop acts on the opening of the bypass valves V11 $_{A/B}$ and V21 $_{A/B}$ to control the temperature at the stack outlet. The second loop acts on the opening of the V0 bypass valve to control the temperature of the water and glycol leaving the WGHE. A PID is assigned to each control

Please cite this article as: Cavo M et al., An advanced control method for fuel cells - Metal hydrides thermal management on the first Italian hydrogen propulsion ship, International Journal of Hydrogen Energy, https://doi.org/10.1016/j.ijhydene.2022.07.223

Table 2 – Installed energy systems on ZEUS.

PEM Fuel Cells [48]		
Installed modules	2	
Installed Power (per module)	71	kW
BOP consumption (at 500A)	11	kW
Nominal operating current	400	A
Minimum operating current	120	A
Maximum current	500	A
Idle current	50	A
Stack efficiency (at 500 A)	47%	
FC system weight	125	kg
Hydrogen storage (MH)		
Installed rack	2	
MH tanks per rack	24	
Hydrogen content per rack	25	kg
Rack dimensions	2.1 × 1.5 x 0.64	m
Rack total weight	3050	kg
Batteries		
Installed modules	84	
Energy per module	1.84	kWh
Efficiency	96%	
Module dimensions	0.31 × 0.22 x 0.17	m
Module weight	19.2	kg

Table 3 – Temperature set points at different working conditions.

Load	TT11 $_{A/B}$ and TT21 $_{A/B}$ [°C]	TT21 and TT22 [°C]
Idle (50 A)	56	54
Minimum operation (120 A)	58	55
Nominal operation (400 A)	64	56
Maximum (500 A)	65	56

signal, which has been calibrated using the Ziegler-Nicolson procedure [56] and then modified to smooth out oscillations and improve responsiveness. Table 4 shows the characteristic coefficients of the controllers in the two loops.

Model predictive control (MPC)

MPC is a model-based control system where a plant model is used to forecast plant status along a moving predicting window, and control outputs are obtained by minimizing a cost function.

In this work, the MPC architecture is based on two functions: one for the discrete model predictive control (DMPC) and one for the observer, according to the velocity form presented by Wang and Young [57]. The model developed for the control is based on augmented state-space representation, i.e., Non-Minimal State Space (NMSS), reported in [58]. The observer is used to estimate the state of the system at each time step, to be fed back to the DMPC dynamic model for the following iteration.

$$\begin{vmatrix} \Delta x_m(k+1) \\ y(k+1) \end{vmatrix} = \begin{vmatrix} A_m & 0_p^T \\ C_m A_m & 1 \end{vmatrix} \begin{vmatrix} \Delta x_m(k) \\ y(k) \end{vmatrix} + \begin{vmatrix} B_m \\ C_m B_m \end{vmatrix} \Delta u(k)$$
$$y(k) = |\, 0_m \quad 1 \,| \begin{vmatrix} \Delta x_m(k) \\ y(k) \end{vmatrix} \tag{3}$$

This non-minimal representation is detectable and stabilizable if the original model is detectable and stabilizable and has no transmission zeros on the unit circle. The integration within the MPC is performed through the application of the Laguerre network and it is used to simplify MPC computation by adding tunable parameters.

One of the advantages of MPC is linked to the possibility to tune controller response based on weights associated to control variables. Here, cost function is based on Discrete Linear Quadratic Regulator (DLQR) architectures, which are used to be as equation (4), with Q and R weight matrices, x is the state of the system, and u is the control signal. DMPC algorithm includes constraints on absolute value of plant inputs u and their rate of change Δu.

$$J = \frac{1}{2} x^T Q x + u^T R u \tag{4}$$

PID defines control signal according to the mismatch of previous time steps, while MPC defines the optimum control signal starting from the current mismatch and predicting the system behavior using the embedded model, minimizing difference between set-point and measured output (equivalent control loop, Fig. 2). Some authors have already explored the integration between the MPC and the fuel cell [59][60], however, this work proposes the comparison between PID and single-input single-output MPC, in two different control loops in stress operating condition for ZEUS thermal system. The V1A fractional opening control allow the monitoring water-glycol outlet temperature of PEMFC modules, while V0 fractional opening control allow the monitoring of water-glycol outlet temperature of WGHE interface exchangers (Fig. 1). Each MPC should embed the NMSS of subsystem of the related control loop, then subsystem of the first MPC includes WGHE-1 and PEMFC Stack 1 A, while the subsystem of the latter MPC includes WGHE-1, MH tanks, and WSHE.

Table 4 – PID constants of ZEUS thermal management system.

PID Constants	First Loop	Second Loop
K_P	2.25	24
K_I	0.06	0.24
K_D	0	0.94

Simulation and results

In this section, the results obtained from the simulations performed on the thermal management system of the integrated PEMFC-MH systems are presented. According to the previous analysis [43], the stability and the effectiveness of the control method through PID in most operation scenarios for the navigation of the ZEUS was verified. In this paper, the two most critical operating scenarios of the ship are investigated: load decrease from nominal to minimum conditions and vice versa (Table 5) by a current ramp speed of 50 A/s (this limit was given by the stacks manufacturer) and PID control logic.

As Fig. 3 shows, the load drop from the nominal to the minimum condition does not lead to critical thermal

Please cite this article as: Cavo M et al., An advanced control method for fuel cells - Metal hydrides thermal management on the first Italian hydrogen propulsion ship, International Journal of Hydrogen Energy, https://doi.org/10.1016/j.ijhydene.2022.07.223

Table 5 – Definition of critical operating conditions under investigation.

	Nominal Power → Minimum Power	Minimum Power → Nominal Power
Current [A]	400 → 120	120 → 400
Gross Electrical Power [kW]	120 → 44	44 → 120
Net Electrical Power [kW]	101 → 38	38 → 101

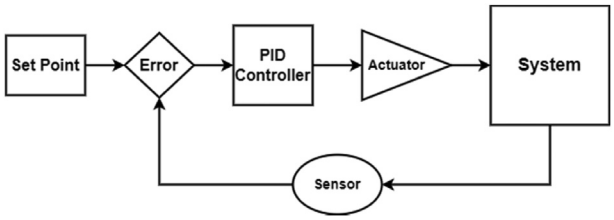

Fig. 3 – Block diagram of a closed loop system controlled by PID.

management of the modules. The lower power consumption corresponds to an increase in stack efficiency and therefore a reduction in heat generation; thus, the cooling flow through the WGHE decreases as the bypass valves open. The maximum temperature deviation recorded is less than 2 °C, which is lower than the set point: therefore, strong load reduction does not cause any thermal problems to the PEMFC control system.

Fig. 4 shows the system's behavior when the 50 A/s current ramp is applied to bring the system from the minimum load operating condition to delivering the nominal power. A significant temperature peak (about 5 °C above the setpoint) occurs, as measured at TT11 $_{A/B}$ and TT21 $_{A/B}$ sensors; also, the system keeps running at a temperature of 2 °C above the set point for more than 37 s. It is mandatory to reduce the latter as much as possible for two reasons: (i) working under adverse temperature conditions decreases the fuel cells lifetime; (ii) a stack alarm system triggers a derating of the power supplied by the modules if this phenomenon lasts more than 60 s.

In conclusion, the PID method system responds to a physical measure of the variable to be controlled and therefore is affected by the dynamics of the two systems in series: in other words, the secondary heating circuit of the hydrides (slower) retards the achievement of a stable equilibrium point of the primary cooling system of the PEMFC modules (quicker). Then, the temperature of the modules takes longer to cool down and the period under critical operating conditions increases. Therefore, it is important to get the secondary circuit control system as fast and stable as possible.

Therefore, this paper investigates possible methods to solve this critical aspect, avoiding temperature peaks and/or extended periods under operating conditions that could affect the lifetime of the PEMFC units. Three solutions are identified and compared with the operating condition suggested by the manufacturer (current ramps at 50 A/s), namely: (i) slow down the current advance speed (manufacturer's suggestion 10 A/s); (ii) introduce an intermediate step; (iii) use an advanced control method such as the MPC.

Ramp at 10 A/s

This section aims to verify if the decrease of the current forward rate to 10A/s, suggested by the manufacturer [46], allows the thermal transient to be easily overcome. The maximum peak temperature has been reduced by 1 °C and the residence time in operating conditions 2 °C above the set point has been limited to 32 s, as can be seen in Fig. 5. Therefore, there is a benefit in terms of both maximum registered temperature and dwell time under critical operating conditions compared to the 50 A/s ramp case. The batteries utilization is limited, as only 0.23 kWh (0.15% of the total SoC) are consumed during the transition step. This solution also highlights the limitation

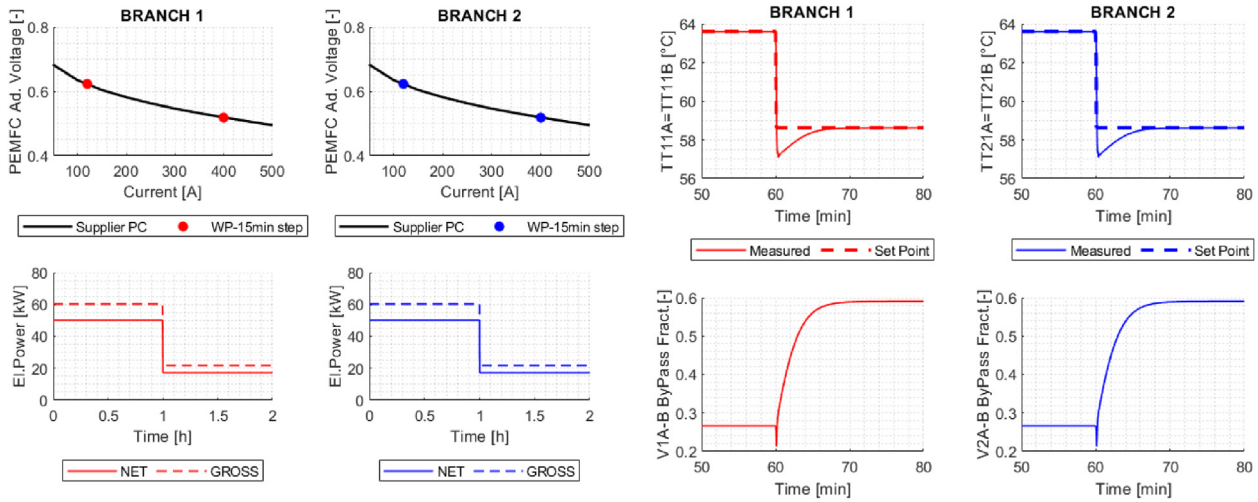

Fig. 4 – Thermal control system behavior of stacks under load decrease from nominal to minimum operating load. Cell voltage scaled to the Nernst voltage and electrical power (left); water-glycol temperature at stack outlet and bypass fraction (right).

Please cite this article as: Cavo M et al., An advanced control method for fuel cells - Metal hydrides thermal management on the first Italian hydrogen propulsion ship, International Journal of Hydrogen Energy, https://doi.org/10.1016/j.ijhydene.2022.07.223

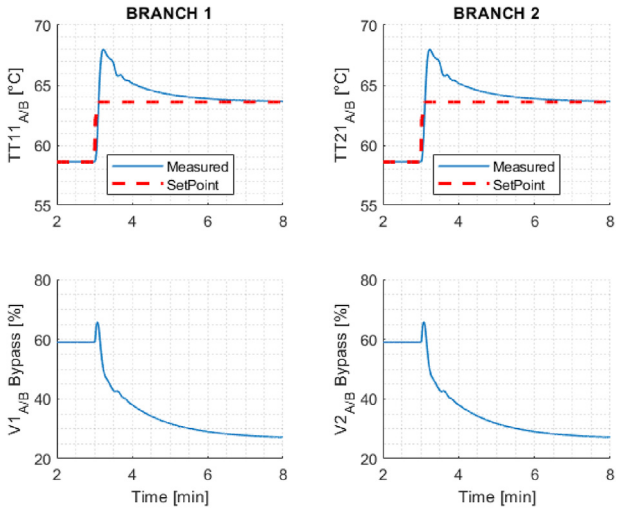

Fig. 5 – Stack outlet temperature of water-glycol and mass fraction of bypass for 50A/s increasing ramp.

of the controller, which is unable to adequately anticipate the control action. Therefore, it is essential to use control systems capable of predicting the dynamic response of the system and anticipating the control action to reduce as much as possible the risk of malfunctioning.

Mid-step solution

In this section, the feasibility of an intermediate step is investigated to reduce the temperature peak during the electrical load advance phase. Therefore, it is reasonable to assume that introducing a short stay in an intermediate load condition would allow the system to dampen the thermal peaks. As Fig. 6 shows, the effect of an intermediate step leads to a drop in the maximum measured temperature (4 °C instead of 5 °C). However, this solution requires more time to reach the desired equilibrium point (around 5 min). As a result, batteries' consumption increases up to 1.45 kWh (1% of the SoC) during the load ramp: although the amount is limited, it can represent a problem if batteries have been fully discharged in previous navigation hours.

Finally, it is important to point out that the maximum dwell time above 2 °C from the setpoint is significantly reduced compared to the previous case (only 11 s).

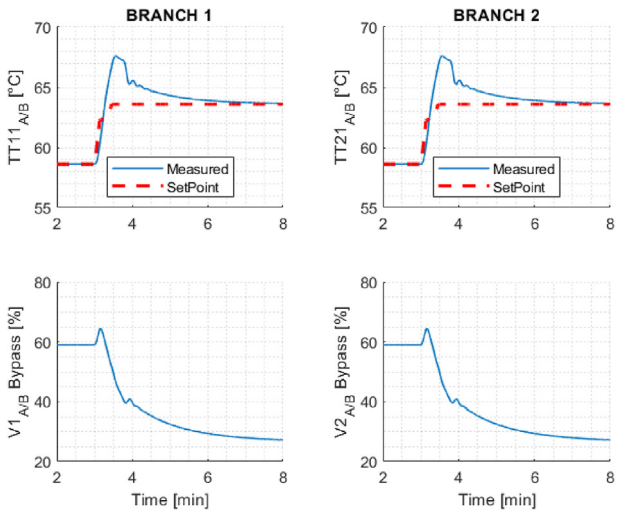

Fig. 6 – Stack outlet temperature of water-glycol and mass fraction of bypass for 10A/s increasing ramp.

MPC

This section describes the results obtained by applying the MPC strategy. The results of the model are analysed by applying a current ramp at both 10 A/s and 50 A/s. The purpose is to verify that the chosen event horizon of MPC and the calibration of the characteristic constants describing the linearized model can shorten the system dwell time at critical conditions (>2 °C than the setpoint). In Fig. 7 it is possible to

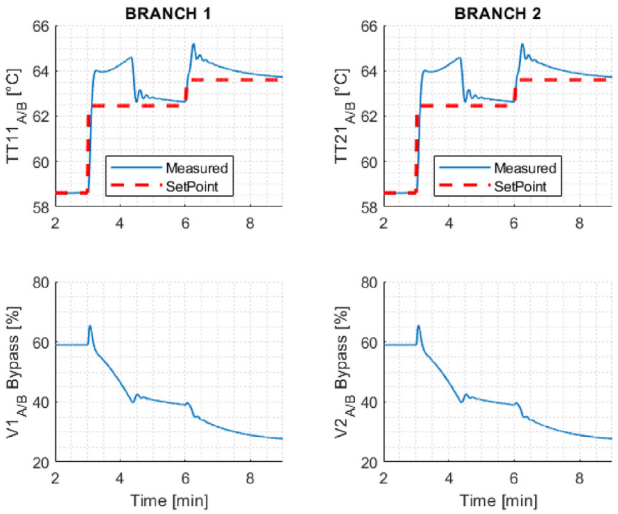

Fig. 7 – Stack outlet temperature of water-glycol and mass fraction of bypass for 50A/s increasing ramp and one mid-step.

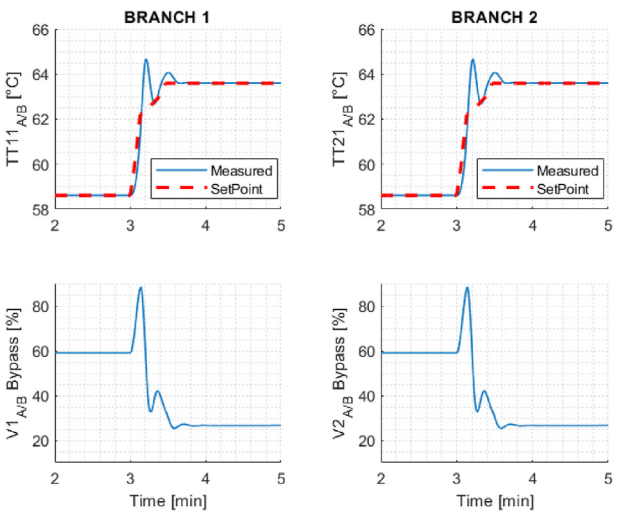

Fig. 8 – Stack outlet temperature of water-glycol and mass fraction of bypass for 10A/s increasing ramp and MPC control method.

Please cite this article as: Cavo M et al., An advanced control method for fuel cells - Metal hydrides thermal management on the first Italian hydrogen propulsion ship, International Journal of Hydrogen Energy, https://doi.org/10.1016/j.ijhydene.2022.07.223

observe that the MPC system reaches the setpoint value avoiding strong temperature peaks and never exceeding the critical temperature threshold. Therefore, it is possible to assert that a current ramp at 10 A/s does not cause any thermal problems in the circuit thanks to the application of MPC logic. Looking at the 50 A/s case, it can be highlighted that the peak temperature recorded has risen slightly (about 6 °C above the setpoint) compared to the PID control (about 5 °C). However, even in this case, the dwell times in critical operating conditions are drastically reduced: only 3 s. Therefore, it is possible to conclude that even the fastest current ramp can be well supported by MPC. Also in this case, battery consumption is very low (<0.1 kWh). It is interesting to highlight that in both cases under analysis, the MPC commands a higher increase of the mass fraction bypassing the WGHE during the initial phase of the step, compared to the PID. It is noticeable how the anticipation of this action plays a fundamental role in allowing the system to overcome thermal transients and bring the circuit to thermal equilibrium sooner (see Fig. 8).

Results comparison

This section compares the techniques used to control the PEMFC and MH thermal management systems onboard the ZEUS. The focus is on the most stressful ramp from the point of view of PEMFC modules: moving from minimum to nominal load. Fig. 9 shows the trend of the cooling temperature $TT_{11\ A/B}$ measured at the stacks' outlet vs time. The dashed line shows the setpoint values. It is interesting to highlight that the 50 A/s ramp with PID is the worst control strategy for PEMFC for this specific case: in fact, there is a sharp temperature peak at the stacks' exit that persists for a long time. A high-temperature peak also occurs when using MPC at 50 A/s, but this control method can bring the system to the new equilibrium point very fast compared to the previous case. The inclusion of an intermediate step by keeping the ramp speed at 50 A/s is a valid solution, which allows both the thermal peaks to be limited and the time spent in non-ideal operating conditions

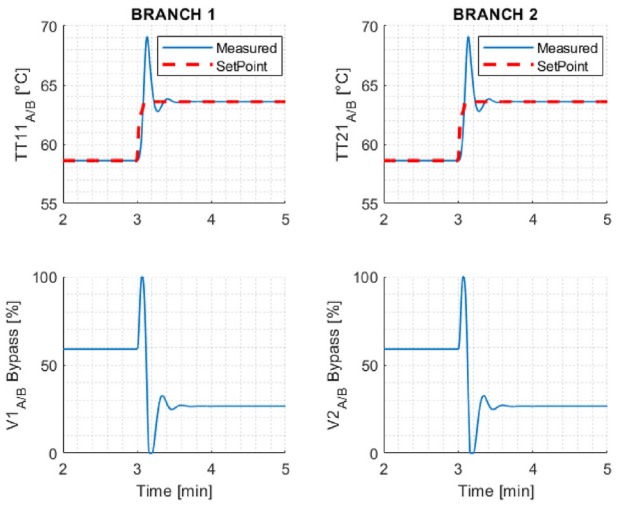

Fig. 9 – Stack outlet temperature of water-glycol and mass fraction of bypass for 50A/s increasing ramp and MPC control method.

Table 6 – Comparison of different control methods in terms of permanence in critical conditions.

Case study	Permanence in critical conditions [s]
50 A/s	37.4
One mid-step at 50 A/s	11
10 A/s	32.8
MPC 50 A/s	2.7
MPC 10 A/s	0

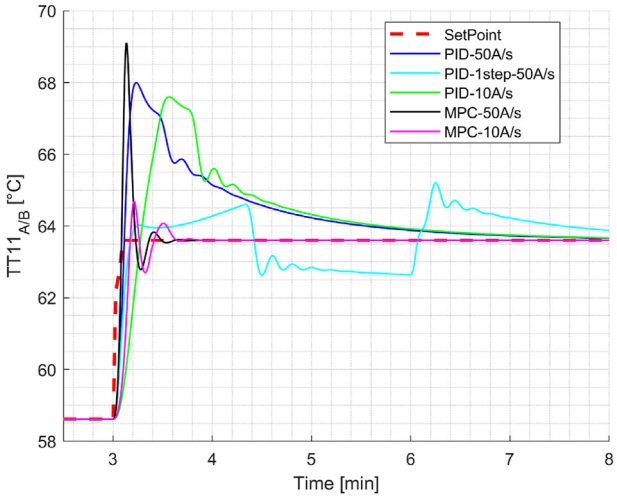

Fig. 10 – Comparison of different control methods and solutions to handle the desired water-glycol outlet temperature of PEMFC modules.

to be minimised; on the other hand, the necessary time to reach the desired working point is the highest in the investigated solutions. Morover, the consumption of the batteries is higher, as they must provide for the lack of PEMFC energy production during the intermediate step. Thus, the case with the application of MPC is presented. The capability of this tool to predict the system's response permits to anticipate the response and eliminate undesired phenomena. In particular, the 10 A/s ramp with MPC manages to handle the load increase very smoothly. On the other hand, applying the MPC control logic to a 50 A/s ramp shows an initial temperature peak, but the system's permanence in critical conditions is considerably reduced (Table 6).

Fig. 10 shows the water-glycol temperature TT_{12} control system at the WGHE outlet. The set point value of this variable (red hatching) is not uniformly ascending with the load, as suggested by the stack manufacturer. All control strategies guarantee a very good level of accuracy. The case with an intermediate step and 50A/s ramp is the only one that shows a more significant deviation, but the error on the target value is still so slight that it does not affect the other system's components. The integrator term of the set-point error in PID effects on the slow response, it integrates the peak set-point mismatch, providing as result the TT_{12} peak late. MPC presents fast response because its control signal is just based on the difference between the real-time measured monitoring parameter and its real-time set-point; if the set-point peak is already passed, MPC does not consider it anymore (see Fig. 11).

Please cite this article as: Cavo M et al., An advanced control method for fuel cells - Metal hydrides thermal management on the first Italian hydrogen propulsion ship, International Journal of Hydrogen Energy, https://doi.org/10.1016/j.ijhydene.2022.07.223

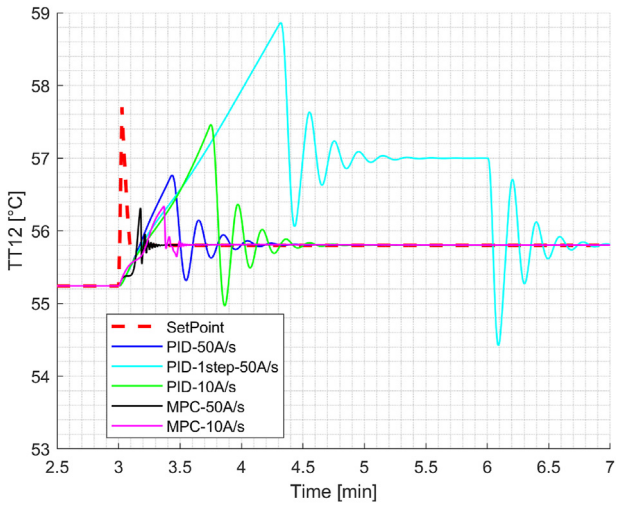

Fig. 11 – Comparison of different control methods and solutions to handle the desired water-glycol outlet temperature of WGHE interface exchangers.

Conclusions

In the present paper, the authors investigated the thermal integration of MH and PEMFC modules for energy propulsion in maritime applications, considering the first Italian hydrogen vessel, named ZEUS and launched in 2022, as real test case.

The proposed approach is based on a Matlab-Simulink model for dynamic analysis of the whole energy system, already developed in previous research by the authors to verify that the heat generated by fuel cells was sufficient to release the required thermal energy amount from MH tanks for the different navigation conditions, including transient ones. A PID control system was considered to guarantee the correct management of the PEMFC cooling system throughout three-way by-pass valve.

In this work, the authors aimed to test the control system in the most critical conditions that can be encountered in navigation, i.e., from minimum to maximum power and vice-versa with a fast ramp (50 A/s) required to fuel cells. This analysis represents a key point for real PEMFC application onboard, as permanence in not desired conditions during transitory can negatively affect their lifetime. Two conditions have been analysed:

- Reduction from nominal (400 A) to minimum (120 A) power: this case does not imply critical conditions, as the deviation from temperature set-point at stacks outlet TT_{11AB} is always lower than 2 °C.
- Increase from minimum (120 A) to nominal (400 A) power: this case presents some issues, as temperature TT_{11AB} shows a peak of 5 °C higher than the set-point; furthermore, a significant time (37 s) is needed to bring the deviation under 2 °C. This can damage PEMFC modules, which are the most expensive components onboard.

To solve this problem, three different strategies have been investigated, achieving the following results:

1. The decrease in the ramp speed to 10 A/s, suggested by PEMFC manufacturer, gives a limited advantage in terms of permanence time in critical conditions (32 s).
2. The introduction of an intermediate step reduces the peak value (4 °C) and the permanence in critical conditions (11 s), on the other hand it requires an energy input from batteries and around 5 min to reach a new equilibrium point.
3. The introduction of an advanced MPC is the best solution, as it allows for a strong reduction in terms of time both in critical operations (2.7 s at 50 A/s, 0 s at 10 A/s) and to reach the new equilibrium point: 48 s for 10 A/s power ramp case and 36 s for 50 A/s power ramp case.

It is worth remarking the general relevance of this paper not only in the framework of the application on the first Italian H2 propelled maritime vessel, but also for the development of robust and safe control systems for the integration of zero-emission energy production fuel cell systems onboard, and their operation at different conditions. The stability of the MPC will be tested in the next future considering the operative load profile that will be tested onboard ZEUS in open sea; the aim is to apply this control logic in Software in the Loop (SiL) and Hardware in the Loop (HiL) mode to the real ship. The developed model represents a key-point for studying and analysing other critical operation conditions for different kind of FCS installed onboard for applications on different ship typologies.

Declaration of competing interest

The authors declare that they have no known competing financial interests or personal relationships that could have appeared to influence the work reported in this paper.

Acknowledgements

This work has been partially supported by Fincantieri S. p.A. and Italian Ministry of Economic Development through the research project TecBia, CUP n. B98I17000680008. The authors gratefully acknowledge A. Dellacasa, M. Romanello and M. Rizzuti for the support and collaboration related to the thermal management circuit.

REFERENCES

[1] International Energy Agency (IEA) official website, https://www.iea.org/reports/global-energy-review-2021/co2-emissions/InternationalEnergyAgency; 22/02/2022.
[2] International Energy Agency (IEA) official website, www.iea.org/data-and-statistics/InternationalEnergyAgency; 22/02/2022.
[3] International Maritime Organization (Imo). Fourth greenhouse Gas study. 2020. available at: www.imo.org.
[4] https://www.imo.org/en/MediaCentre/HotTopics/Pages/Reducing-greenhouse-gas-emissions-from-ships.aspx, International Maritime Organization (IMO) official website, last access 22/01/2021.
[5] Maritime forecast to 2050-Energy transition outlook. DNV-GL Maritime; 2019.

Please cite this article as: Cavo M et al., An advanced control method for fuel cells - Metal hydrides thermal management on the first Italian hydrogen propulsion ship, International Journal of Hydrogen Energy, https://doi.org/10.1016/j.ijhydene.2022.07.223

[6] Setting the course to low carbon shipping. American Bureau of Shipping (ABS); 2019.
[7] Huang M, He W, Incenik A, Cichon A, Królczyk G, Li Z. Renewable energy storage and sustainable design of hybrid energy powered ships: a case study. J Energy Storage 2021;43:103266. https://doi.org/10.1016/j.est.2021.103266.
[8] Ampah JD, Yusuf AA, Afrane S, Jin C, Liu H. Reviewing two decades of cleaner alternative marine fuels: towards IMO's decarbonization of the maritime transport sector. J Clean Prod 2021;320:128871. https://doi.org/10.1016/j.jclepro.2021.128871.
[9] Al-Enazi A, Okonkwo EC, Bicer Y, Al-Ansari T. A review of cleaner alternative fuels for maritime transportation. Energy Rep 2021;7:1962–85. https://doi.org/10.1016/j.egyr.2021.03.036.
[10] McKinlay CJ, R: Turnock S, Hudson DA. Route to zero emission shipping: hydrogen, ammonia or methanol? Int J Hydrogen Energy 2021;46:28282–97. https://doi.org/10.1016/j.ijhydene.2021.06.066.
[11] Nuchturee C, Li T, Xia H. Energy efficiency of integrated electric propulsion for ships – a review. Renew Sustain Energy Rev 2020;134:110145. https://doi.org/10.1016/j.rser.2020.110145.
[12] Ammar NR, Seddiek IS. Enhancing energy efficiency for new generations of containerized shipping. Ocean Eng 2020;215:107887. https://doi.org/10.1016/j.oceaneng.2020.107887.
[13] Fokkema JE, Buijs P, Vis IFA. An investment appraisal method to compare LNG-fueled and conventional vessels. Transportation Research, Transport Environ. 2017;56:229–40.
[14] Ammar NR. *An environmental and economic analysis of methanol fuel for a cellular container ship*, Transportation Research. Transport Environ 2019;69:66–76.
[15] Inal OB, Zincir B, Deniz C. Investigation on the decarbonization of shipping: an approach to hydrogen and ammonia. Int J Hydrogen Energy 2022;47:19888–900. https://doi.org/10.1016/j.ijhydene.2022.01.189.
[16] Ye M, Sharp P, Brandon N, Kucernak A. System-level comparison of ammonia, compressed and liquid hydrogen as fuels for polymer electrolyte fuel cell powered shipping. Int J Hydrogen Energy 2022;47:8565–84. https://doi.org/10.1016/j.ijhydene.2021.12.164.
[17] Bicer Y, Dincer I. Environmental impact categories of hydrogen and ammonia driven transoceanic maritime vehicles: a comparative evaluation. Int J Hydrogen Energy 2018;43:4583–96. https://doi.org/10.1016/j.ijhydene.2017.07.110.
[18] De-Troya JJ, Alvarez C, Fernàndez-Garrido C, Carral L. Analysing the possibilities of using fuel cells in ships. Int J Hydrogen Energy 2016;41:2853–66. https://doi.org/10.1016/j.ijhydene.2015.11.145.
[19] van Biert L, Godjevac M, Visser K, Aravind PV. A review of fuel cell systems for maritime applications. J Power Sources 2016;327:345–64. https://doi.org/10.1016/j.jpowsour.2016.07.007.
[20] Inal OB, Deniz C. Assessment of fuel cell types for ships: based on multi-criteria decision analysis. J Clean Prod 2020;265:121734. https://doi.org/10.1016/j.jclepro.2020.121734.
[22] Rivarolo M, Rattazzi D, Magistri L. Best operative strategy for energy management of a cruise ship employing different distributed generation technologies. Int J Hydrogen Energy 2018;43:23500–10. https://doi.org/10.1016/j.ijhydene.2018.10.217.
[23] Rivarolo M, Rattazzi D, Lamberti T, Magistri L. Clean energy production by PEM fuel cells on tourist ships: a time-dependent analysis. Int J Hydrogen Energy 2020;45:25747–57. https://doi.org/10.1016/j.ijhydene.2019.12.086.
[24] Letafat A, et al. An efficient and cost-effective power scheduling in zero-emission ferry ships, complexity, special issue complexity, dynamics, control, and applications of nonlinear systems with multistability. 2020. https://doi.org/10.1155/2020/6487873.
[25] Choi CH, et al. Development and demonstration of PEM fuel-cell-battery hybrid system for propulsion of tourist boat. Int J Hydrogen Energy 2016;41:3591–9. https://doi.org/10.1016/j.ijhydene.2015.12.186.
[26] Bassam AM, Phillips AB, R: Turnock S, Wilson PA. Development of a multi-scheme energy management strategy for a hybrid fuel cell driven passenger ship. Int J Hydrogen Energy 2017;42:623–35. https://doi.org/10.1016/j.ijhydene.2016.08.209.
[27] Klebanoff LE, et al. Comparative study of a hybrid research vessel utilizing batteries or hydrogen fuel cells. Int J Hydrogen Energy 2021;46:38051–72. https://doi.org/10.1016/j.ijhydene.2021.09.047.
[28] Wu P, Bucknall R. Hybrid fuel cell and battery propulsion system modelling and multi-objective optimization for a coastal ferry. Int J Hydrogen Energy 2020;45:3193–208. https://doi.org/10.1016/j.ijhydene.2019.11.152.
[29] Li X, Han K, Song Y. Dynamic behaviors of PEM fuel cells under load changes. Int J Hydrogen Energy 2020;39:20312–20. https://doi.org/10.1016/j.ijhydene.2019.12.034.
[30] Bagherabadi KM, Skjong S, Pedersen E. Dynamic modelling of PEM fuel cell system for simulation and sizing of marine power systems. Int J Hydrogen Energy 2022;47:17699–712. https://doi.org/10.1016/j.ijhydene.2022.03.247.
[31] Hu K, Chu T, Li F, Wang B, Zhang Z, Liu T. Effect of different control strategies on rapid cold start-up of a 30-cell proton exchange membrane fuel cell stack. Int J Hydrogen Energy 2021;46:31788–97. https://doi.org/10.1016/j.ijhydene.2021.07.041.
[32] Gadducci E, Lamberti T, Bellotti D, Magistri L, Massardo AF. BoP incidence on a 240 kW PEMFC system in a ship-like environment, employing a dedicated fuel cell stack module. Int J Hydrogen Energy 2021;46:24305–17. https://doi.org/10.1016/j.ijhydene.2021.04.192.
[33] Gadducci E, Lamberti T, Rivarolo M, Magistri L. Experimental campaign and assessment of a complete 240-kW Proton Exchange Membrane Fuel Cell power system for maritime applications. Int Journal of Hydrogen Energy 2022;47:22545–8.
[34] Nascimiento AL, Yahyaoui I, Fardin JF, Encarnação LF, Tadeo F. Modeling and experimental validation of a PEM fuel cell in steady and transient regimes using PSCAD/EMTDC software. Int J Hydrogen Energy 2020;45:30870–81. https://doi.org/10.1016/j.ijhydene.2020.04.184.
[35] Barthelemy H, Weber M, Barbier F. Hydrogen storage: recent improvements and industrial perspectives. Int J Hydrogen Energy 2017;42:7254–62. https://doi.org/10.1016/j.ijhydene.2016.03.178.
[36] Moradi R, Groth KM. Hydrogen storage and delivery: review of the state of the art technologies and risk and reliability analysis. Int J Hydrogen Energy 2019;44(23):12254–69. https://doi.org/10.1016/j.ijhydene.2019.03.041.
[37] Lototskyy MV, Tolj I, Pickering L, Sita C, Barbir F, Yartys V. The use of metal hydrides in fuel cell applications. Prog Nat Sci: Mater Int 2017;27:3–20.
[38] Nguyen HQ, Shabani B. Review of metal hydride hydrogen storage thermal management for use in the fuel cell systems. Int J Hydrogen Energy 2022;46:7738–45. https://doi.org/10.1016/j.ijhydene.2021.07.057.
[39] von Colbe JB, et al. Application of hydrides in hydrogen storage and compression: achievements, outlook and perspectives. Int J Hydrogen Energy 2019;44:7780–808.

Please cite this article as: Cavo M et al., An advanced control method for fuel cells - Metal hydrides thermal management on the first Italian hydrogen propulsion ship, International Journal of Hydrogen Energy, https://doi.org/10.1016/j.ijhydene.2022.07.223

[40] Fiori C, Dell'Era A, Zuccari F, Santiangeli A, D'Orazio A, Orecchini F. Hydrides for submarine applications: overview and identification of optimal alloys for air independent propulsion maximization. Int J Hydrogen Energy 2015;40:11879–89.
[41] Chabane D, Ibrahim M, Harel F, Djerdir A, Candusso D, Elkedim O. Energy management of a thermally coupled fuel cell system and metal hydride tank. Int J Hydrogen Energy 2019;44:27553–63. https://doi.org/10.1016/j.ijhydene.2019.08.247.
[42] Rizzi P, Pinatel E, Luetto C, Florian P, Graizzaro A, Gagliano S, Baricco M. Integration of a PEM fuel cell with a metal hydride tank for stationary applications. J Alloys Compd 2015;645:338–42. https://doi.org/10.1016/j.jallcom.2014.12.145.
[43] Cavo M, Gadducci E, Rattazzi D, Rivarolo M, Magistri L. Dynamic analysis of PEM fuel cells and metal hydrides on a zero-emission ship: a model-based approach. Int J Hydrogen Energy 2021;46:32630–44. https://doi.org/10.1016/j.ijhydene.2021.07.104.
[44] https://www.energy-observer.org/ lastaccess15/03/2022.
[45] https://ec.europa.eu/environment/life/project/Projects/index.cfm?fuseaction=home.showFile&rep=file&fil=Zemships_Brochure_EN.pdf. [Accessed 15 March 2022].
[46] https://www.switchmaritime.com/tech. [Accessed 15 March 2022].
[47] https://fuelcellsworks.com/news/europe/proton-motor-power-systems-receives-additional-order-from-fincantieri-for/lastaccess. [Accessed 15 February 2021].
[48] Private Communication by ProtonMotor https://www.proton-motor.de/.
[49] https://www.gknhydrogen.com/.
[50] https://www.lithionbattery.com/products/modules/.
[52] Baroud Z, Benmiloud M, Benalia A, Ocampo-Martinez C. Novel hybrid fuzzy-PID control scheme for air supply in PEM fuel-cell-based systems. Int J Hydrogen Energy 2017;42:10435–47. https://doi.org/10.1016/j.ijhydene.2017.01.014.
[53] Sharma S, Babu GUB. A new control strategy for a higher order proton exchange membrane fuel cell system. Int J Hydrogen Energy 2020;45:25945–59. https://doi.org/10.1016/j.ijhydene.2020.05.140.
[54] Mantelli L, Ferrari ML, Traverso A. Dynamics and control of a turbocharged solid oxide fuel cell system. Appl Therm Eng 2021;191:116862. https://doi.org/10.1016/j.applthermaleng.2021.116862.
[55] Ou K, Wang Y, Li Z, Shen Y, Xuan D. Feedforward fuzzy-PID control for air flow regulation of PEM fuel cell system. Int J Hydrogen Energy 2015;40:11686–95. https://doi.org/10.1016/j.ijhydene.2015.04.080.
[56] Goodwin G, Graebe S, Salgado M. Control system design. Valparaiso: Prentice Hall; 2000.
[57] Wang L, Young PC. An improved structure for model predictive control using non-minimal state space realisation. J Process Control 2006;16:355–71.
[58] Wang L. Model predictive control system design and implementation using MATLAB®. Advances in industrial control. Springer London; 2009. https://doi.org/10.1007/978-1-84882-331-0.

Please cite this article as: Cavo M et al., An advanced control method for fuel cells - Metal hydrides thermal management on the first Italian hydrogen propulsion ship, International Journal of Hydrogen Energy, https://doi.org/10.1016/j.ijhydene.2022.07.223